Acta Oceanol. Sin., 2014, Vol. 33, No. 12, P. 1–14
DOI: 10.1007/s13131-014-0567-6
http://www.hyxb.org.cn
E-mail: hyxbe@263.net

An evaluation of the simulations of the Arctic Intermediate Water in climate models and reanalyses

LI Xiang[1,2], SU Jie[1]*, ZHAO Jinping[1]

[1] Key Laboratory of Physical Oceanography, Ocean University of China, Qingdao 266100, China
[2] Key Laboratory of Ocean Circulation and Wave, Institute of Oceanology, Chinese Academy of Sciences, Qingdao 266071, China

Received 28 March 2014; accepted 19 June 2014

Abstract

The simulations of the Arctic Intermediate Water in four datasets of climate models and reanalyses, CCSM3, CCSM4, SODA and GLORYS, are analyzed and evaluated. The climatological core temperatures and depths in both CCSM models exhibit deviations over 0.5°C and 200 m from the PHC. SODA reanalysis reproduces relatively reasonable spatial patterns of core temperature and depth, while GLORYS, another reanalysis, shows a remarkable cooling and deepening drift compared with the result at the beginning of the dataset especially in the Eurasian Basin (about 2°C). The heat contents at the depth of intermediate water in the CCSM models are overestimated with large positive errors nearly twice of that in the PHC. To the contrary, the GLORYS in 2009 show a negative error with a similar magnitude, which means the characteristic of the water mass is totally lost. The circulations in the two reanalyses at the depth of intermediate water are more energetic and realistic than those in the CCSMs, which is attributed to the horizontal eddy-permitting resolution. The velocity fields and the transports in the Fram Strait are also investigated. The necessity of finer horizontal resolution is concluded again. The northward volume transports are much larger in the two reanalyses, although they are still weak comparing with mooring observations. Finally, an investigation of the impact of assimilation is done with an evidence of the heat input from assimilation. It is thought to be a reason for the good performance in the SODA, while the GLORYS drifts dramatically without assimilation data in the Arctic Ocean.

Key words: Arctic Intermediate Water, model evaluation, Arctic modeling, impact of data assimilation

Citation: Li Xiang, Su Jie, Zhao Jinping. 2014. An evaluation of the simulations of the Arctic Intermediate Water in climate models and reanalyses. Acta Oceanologica Sinica, 33(12): 1–14, doi: 10.1007/s13131-014-0567-6

1 Introduction

The Arctic Ocean is an indicator of the climate change and has the most active responses to the global warming event (Intergovernmental Panel on Climate Change, the fourth IPCC assessment report) (Pachauri and Reisinger, 2007). The Arctic Intermediate Water (AIW), also named the Atlantic Water (AW) layer in the Arctic Ocean, occupies the 150–1 000 m depth of the water column throughout the Arctic Ocean. The unique characteristic of this water mass is a relatively high temperature above 0°C. Although the upward heat flux is restricted to only several watts per square meter in the Arctic Basin by virtue of the halocline above (Steele and Boyd, 1998; Rudels et al., 1996), the influence of AIW on the distribution of sea ice does exist (Polyakov et al., 2004; Polyakov et al., 2011; Ivanov et al, 2012). The huge heat content stored in the AIW, which could melt all the sea ice in the Arctic Ocean if released to the surface (Polyakov et al., 2011), is a potential factor of the climate change.

The Atlantic water enters the Arctic Ocean by two pathways from the Greenland-Iceland-Norwegian (GIN) Seas. The warmer branch named the Fram Strait Branch (FSB) goes through the deep Fram Strait. The other one called the Barents Sea Branch (BSB) goes by the shallow Barents Sea Opening. The latter branch undergoes significant transformation processes due to active air-sea exchange in shallow shelf seas, i.e., the Barents Sea and the Kara Sea. This branch of Atlantic-origin water is cooler and fresher than the FSB when they meet at the St. Anna Trough (e.g., Rudels et al., 1994). Both branches flow at the intermediate depth around the Arctic Basin cyclonically, forming the Arctic Circumpolar Boundary Current (ACBC) (Rudels et al., 1999; Aksenov et al., 2011).

Owing to lack of observations, the Arctic Ocean is not fully understood especially under the surface (e.g., Rudels et al., 2013). So the models become an important tool for investigating the physical processes in the Arctic Ocean. However, the simulated AIW suffers significant deviations in ocean general circulation models. Holloway et al. (2007) summarized the performances of the Arctic Ocean Model Intercomparison Project (AOMIP) on water properties and ocean circulation which showed that most of the simulated AIWs were either too warm or cold and/or at unrealistic depths. Although the biases of the AIW were mentioned with some tentative investigations by some researchers (e.g., Lique and Steele, 2012; Li et al., 2013), a comprehensive description of performance and reproducibility of the AIW in present reanalysis data and model results has not been given so far.

In this paper, we will focus on the simulations of the AIW in

Foundation item: The National Basic Research Program (973 Program) of China under contract No. 2013CBA01805; the National Natural Science Foundation of China under contract No. 41330960; the Plan 111 of Ocean University of China under contract B07036.
*Corresponding author, E-mail: sujie@ouc.edu.cn

four datasets including coupled climate models and reanalyses with data assimilation. The reasons for the deviations among the datasets will be analyzed briefly. The paper is arranged as follows: a short description of datasets will be shown in Section 2; climatological spatial patterns and heat contents of the AIW will be illustrated in Section 3; the discussions of the reasons for the biases will be done in Sections 4 and 5.

2 Datasets

In this section, general information for data used in the study will be shown. The datasets include hydrography climatology, reanalyses with data assimilation and output of climate models. Based on the focus of this paper, a brief description of the ocean models will be stated particularly with some important characters listed in Table 1, while many other details will be omitted, as can be obtained from the documents or websites of these datasets.

2.1 *Polar hydrographic climatology (PHC)*

The lack of *in situ* observations is a particular reality for researchers on the Arctic Ocean. The ice cover on the surface prevents the data from satellites' origin. Fortunately, a gridded climatological hydrography dataset PHC with a high quality in the Arctic Ocean was created at the University of Washington (Steele et al., 2001). It merges the World Ocean Atlas (WOA) from the National Oceanographic Data Center (NODC), the Arctic Ocean Atlas (AOA) from Environmental Working Group (EWG) and some Canadian observations from the Bedford Institute of Oceanography (BIO). The PHC has been the most reliable thermohaline data in the Arctic Ocean solely based on observations so far. Its spatial resolution is 1°, the same as the WOA. The depths of vertical layers are also identical to the WOA with 33 layers down to 5 500 m. In this study, the latest version PHC 3.0 is used, which had been updated till the year 2005.

As a result, the PHC is treated as an objective criterion in evaluating the spatial patterns of temperature and salinity of the modeled outputs. Note that it does not mean the PHC is perfect, since the observations are very inhomogeneous both temporally and spatially.

2.2 *Community climate system model (CCSM)*

CCSM is a climate model composed of four separate models of atmosphere, ocean, sea ice and land developed in the National Center for Atmospheric Research (NCAR). It is a representative coupled model in the coupled model inter comparison project (CMIP), which was established by the working group on coupled modeling (WGCM) in order to compare and study the output from coupled climate models. Many studies using the CMIP model simulations were important scientific evidences included in the assessment report (AR) of the IPCC. In this paper, two versions of the CCSM output are used, the CCSM3 and CCSM4, which are the participants in the CMIP3 and CMIP5, respectively.

The CCSM3 is an open-source climate model for researchers released in 2004 (Collins et al., 2006). The ocean part is the parallel ocean program (POP 1.4.3) with a typical non-eddy-permitting horizontal resolution of nominal 1°. Owing to the huge amount of calculation from each component, climate models usually adopt coarse horizontal grids. The nominal 1° grid is in common use for CMIP/IPCC models, meaning a non-eddy-permitting grid for the polar region since the Rossby deformation radius is *O* (10 km) in the Arctic Ocean. Main parameterizations and techniques include implicit free surface, virtual surface salt flux, GM90 eddy parameterization (Gent and McWilliams, 1990), anisotropic horizontal viscosity with Smagorinsky-type coefficients (e.g., Smith and McWilliams, 2003), non-local K-Profile parameterization (KPP) vertical mixing with some modifications (Large et al., 1994), solar penetration and river mouth mixing treatment. The CCSM4 is a new version of the CCSM climate model with improvements mainly on the ocean physics. The horizontal resolution is not intensified, while the number of vertical layers increases to 60 from 40 in the CCSM3, suggesting an improved capability of reproducing physical processes at subsurface and intermediate depth. The simulations of both CCSM simulations used here are historical 20th century scenario runs.

2.3 *Simple ocean data assimilation (SODA)*

SODA is an ocean reanalysis product from the Texas A&M University (Carton and Giese, 2008). The ocean is manipulated by an ocean general circulation model with continuous assimilation of observations. The ocean physics is under the POP framework with a 0.25°×0.4° horizontal resolution, which is an eddy-permitting resolution for global and polar regions. Main parameterizations contain KPP mixing, biharmonic lateral mixing, and prognostic sea level by a linearized continuity equation. It is worth noting that the sources of assimilation include the data of the Arctic Ocean, which is a distinctive characteristic and allows us to analyze the physical processes in the Arctic Ocean.

2.4 *Global ocean reanalysis and simulations (GLORYS)*

GLORYS is a joint European project of reanalysis product led by MERCATOR-Ocean, France (Ferry et al., 2012). The ocean engine of this product is NEMO (Nucleus for European Modeling of the Ocean (Madec, 2008). The horizontal grid is ORCA025, a tripolar nominal (1/4)° curvilinear grid made by the NOC (National Oceanography Centre, UK). Like the SODA, it is also an eddy-permitting reanalysis with data assimilation. The water column is divided into 75 layers vertically, which gives a chance to resolve complex physical processes at the upper and intermediate layer. Main parameterizations of the GLORYS2 include TKE (turbulent closure scheme) vertical mixing, biharmonic viscosity for momentum, isopycnal diffusion for tracers, partial step for the bottom topography, and filtered free surface. Note that the assimilation data of the GLORYS do not include the Arctic Ocean, which is a sensitive factor in this study (see Ferry et al., 2012 for assimilation data source in detail).

3 Climatological performances

3.1 *Criteria for evaluation*

The AIW is characterized by its high temperature at the intermediate depth. Here we adopt a commonly used representative benchmark (Polyakov et al., 2004), Arctic Intermediate Water core temperature (AIWCT), to evaluate the simulations of modeled results and reanalysis data. AIWCT is defined by the maximum temperature below halocline (i.e., pycnocline) in a vertical profile. Since the heat content of the AIW originates from the North Atlantic Ocean, the core temperature represents the most unchanged part of the Atlantic water. So the AIWCT is a good tracer for the movement of Atlantic water, and the cir-

Table 1. Basic information of modeled datasets

	CCSM3	CCSM4	SODA	GLORYS
Version	CMIP3	CMIP5	2.1.6	2-R20110216
Horizontal resolution	nominal 1°	nominal 1°	0.25°×0.4°	nominal 0.25°
Vertical partition (layers)	40	60	40	75
Temporal range for constructing climatology	1958–1999	1958–2005	1958–2006	1993–2009
Data assimilation	no	no	yes	yes, without Arctic Ocean
Vertical mixing	KPP	KPP	KPP	TKE
Horizontal viscosity	Smagorinsky-harmonic	Smagorinsky-harmonic	biharmonic	biharmonic
Horizontal diffusion	GM90	GM90	biharmonic	GM90

culation at the intermediate depth is usually deduced according to the spatial distribution of the AIWCT (e.g., Rudels et al., 1994), since the direct measurements of velocity are rare. In other papers, the AIWCT is sometimes named Atlantic water core temperature (AWCT) or Intermediate Water core temperature (IWCT) (Polyakov et al., 2004; Li et al., 2011; Li et al., 2012), with the same meaning. The depth of the AIWCT is usually called the (Arctic) Intermediate Water Core Depth (AIWCD/ IWCD)(Li et al., 2012; Zhong and Zhao, 2014), reflecting the vertical position of this water mass.

The Arctic Ocean is divided into four basins by three ridges, Gakkel Ridge, Lomonosov Ridge and Alpha-Mendeleev Ridge (Fig. 1). The distribution and movement of the AIW are influenced by the constraint of topography significantly (Rudels et al., 2004). The seasonal variability of the AIW can be omitted at most parts of the Arctic Ocean (Lique and Steele, 2012) and is not taken into account in this paper. A reference of the spatial AIWCT distribution based on the PHC annual climatology is shown in Fig. 2. Here the maximum temperature below 100 m in the water column is selected as the AIWCT according to the fact that other water masses are much colder. The region is left blank where the depth of the maximum temperature is shallower than 100 m. This is a reasonable cutoff value because the the AIWCD is about 250–500 m in the Arctic interior (Li, 2008; see also Fig. 2b). The spatial patterns of the AIWCT and the AIWCD can directly reflect the reproducibility of the AIW of datasets and will be illustrated in the next section.

In fact, the extreme value AIWCT may be affected by the vertical discretization of model layers and discrepancies in the vertical diffusion. Another benchmark, the heat content of the whole AIW column, is also utilized in the interest of a quantitative description of the whole AIW column. We divide the Arctic

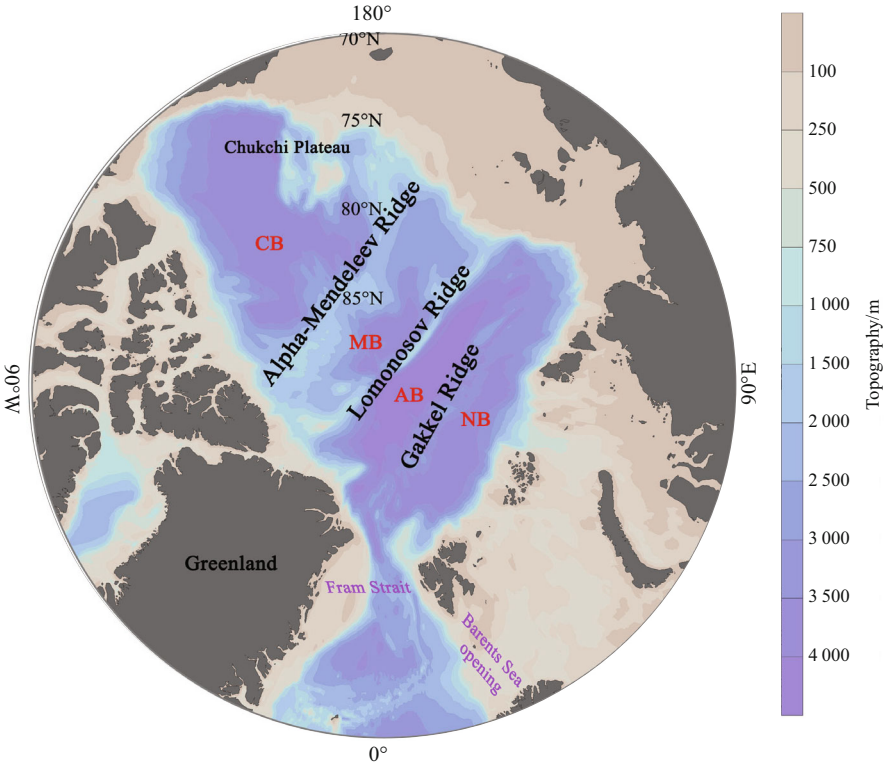

Fig.1. Topography of the Arctic Ocean. The abbreviations of four basins NB, AB, MB and CB represent the Nansen Basin, the Amundsen Basin, the Makarov Basin and the Canada Basin, respectively.

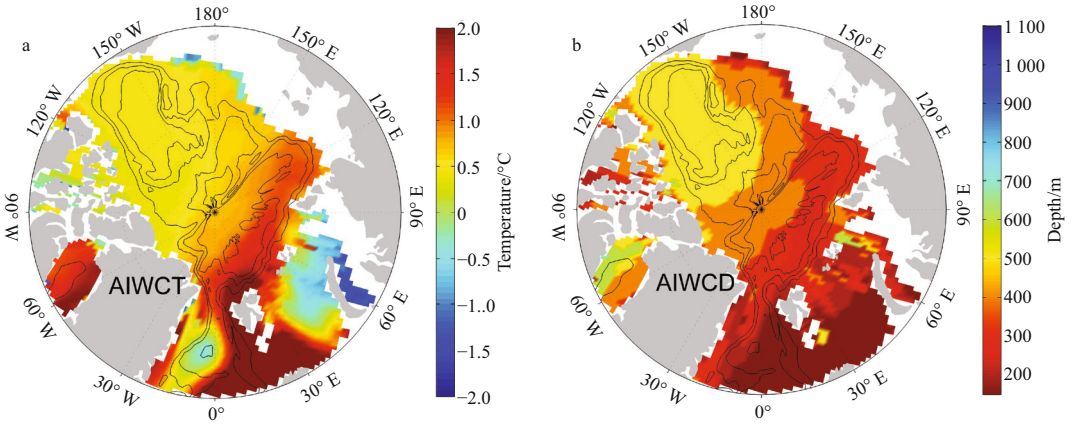

Fig.2. Spatial distributions of Arctic Intermediate Water core temperature (AIWCT) (a) and depth (AIWCD) (b) based on PHC3 annual climatology. Black lines are isobaths of 1 500, 2 500 and 3 500 m.

Ocean into nine partitions artificially but geographically in order to evaluate the reproducibility of data in each region (Fig. 3). And this treatment also has the benefit of examining the pathway of transport of the AIW in the Arctic Ocean.

All data are climatological annual mean values except for the GLORYS, which has a significant cooling trend. And again, the heat content of AIW of the PHC is chosen as the reference value. The calculation has several steps as follows.

(1) A weighted average temperature profile of each partition b is computed using the weight of grid area A. Then we obtain the profile T_b in each partition of every dataset (PHC, CCSM3, CCSM4, SODA, GLORYS1993 and GLORYS2009),

$$T_b = \frac{\sum_b T_i A_i}{\sum_b A_i} .$$

(2) Difference of heat content referring to PHC from 100 to 1 000 m in each partition is integrated. The integration uses trapezoidal method from the interpolated profiles with 1 m-interval. c_p and ρ_0 are specific heat and density of sea water, respectively.

$$d_{\mathrm{ch}} = c_p \rho_0 \int_{100}^{1000} \left(T_{\mathrm{mod}} - T_{b,\mathrm{phc}}\right) \mathrm{d}z .$$

(3) A reference heat content of PHC is calculated referring to 0°C (a typical temperature to distinguish AIW).

$$C_{h,\mathrm{phc}} = c_p \rho_0 \int_{100}^{1000} \left(T_{b,\mathrm{phc}} - T_{\mathrm{r}}\right) \mathrm{d}z \text{ , for } T_{b,\mathrm{phc}} > T_{\mathrm{r}} \text{ and } T_{\mathrm{r}} = 0.$$

(4) Then the relative error of heat content e_{r} is obtained in each partition,

$$e_{\mathrm{r}} = d_{\mathrm{ch}} / C_{h,\mathrm{phc}} .$$

For the Atlantic water layer in the Arctic Ocean is usually defined as the water with temperature above 0, this relative error can give us a direct sense that to what extent the data drift. The performances of the heat content of datasets will be compared in the next section.

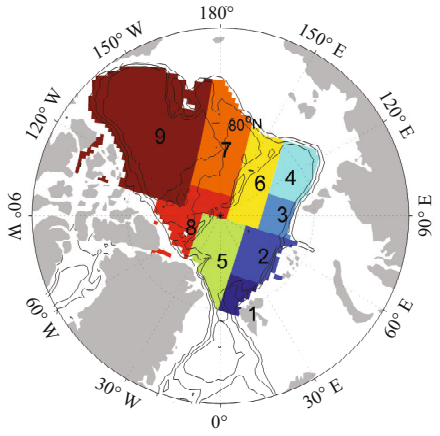

Fig.3. Partition of the Arctic Ocean. Partitions 1–4 represent Nansen Basin from the west to the east; 5–6 Amundsen Basin; 7–8 Makarov Basin; 9 Canada Basin. Partition 10 in the text means the whole Arctic Basin.

3.2 *AIWCT and AIWCD in the PHC*

The most significant spatial characteristic of the AIW is the differences among four basins. The AIWCT is the highest at its entrance, the Fram Strait. And it gets cooler inside in light of its distance away from the entrance. The Atlantic Water is the warmest in the Nansen Basin with a core temperature about 1.5°C, while it is a little less than 1°C in the Amundsen Basin. After crossing the Lomonosov Ridge, the AIWCT keeps on declining and becomes coldest in the Canada Basin where the AIWCT is slightly below 0.5°C. Core temperature seems relatively uniform in each basin. That is to say, the AIW does not suffer significant heat loss from mixing along its track of several thousand kilometers in the Nansen Basin. Figure 2 also reveals the

different fates of the two branches of the ACBC. The FSB maintains its warm characteristic after passing the Fram Strait as the main heat source at the intermediate depth probably, while the BSB loses most of its heat content in the shelf Barents Sea. The Atlantic water undergoes notable transformation along its meandering track in the Barents Sea and the Kara Sea. As a result, the core temperature of the BSB decreases to almost 0°C in the St. Anna Trough, where this branch meets the FSB and joins the ACBC. It is easy to see that the BSB cannot supply the core temperature in the Nansen Basin for its rather low temperature. This is also supported by Wang et al. (2008), whose modeled results show that 89% of the heat content of BSB is lost before it reached the St. Anna Trough. Actually, the thermal structure in the St. Anna Trough is complex with significant heat loss of the FSB (Dmitrenko et al., 2014). The 1-degree PHC is not able to resolve this phenomenon, as is an intrinsic discrepancy.

The spatial pattern of the AIWCD based on the PHC is similar to some extent (Fig. 2b) with shallowest place in the Nansen Basin and deepest place in the Canada Basin. However, the depth of the AIW is a complicated question, as has not been totally comprehended yet. The water mass tends to move along the isopycnal surface, while the thermohaline structure is not uniform horizontally in the upper Arctic Ocean with significant differences between the Eurasian Basin and the Amerasian Basin (Rudels et al., 2004). The sea surface salinity in the Eurasian Basin is much higher, and the winter mixed layer can be produced as a uniform layer of temperature and salinity as a result of the haline convection caused by the ice formation process. So the isopycnal surface of the Atlantic Water is relatively shallow in this part of the Arctic Ocean. Nevertheless, in the Amerasian Basin, there is a big freshwater reservoir, the Beaufort Gyre in the Canada Basin, which is known as one of the main characteristics of the upper Arctic circulation. Driven by the Beaufort High above, the water moves anticyclonically and assembles freshwater from river runoff and fresh Pacific-origin water, forming a quite fresh upper layer in the Canada Basin. This unique thermohaline structure suppresses the halocline so the AIW must be at a deeper position than that in the Eurasian Basin. The circulation of the Atlantic Water in the Canada Basin may be not stable as imagine, and is in debate at present (Karcher et al., 2012). Also, there are at least three pathways for the Atlantic water inferred by observations (McLaughlin et al., 2009). In spite of some unsolved reasons, knowledge of the AIWCD based on the PHC will be considered as a criterion in the rest part of the paper.

3.3 *AIWCT and AIWCD in modeled datasets*

The AIWCT of the CCSM3 shows significant deviations from the PHC (Figs 4a and c). The characteristic of tracer of Atlantic water diminishes in the CCSM3 with no marked spatial struc-

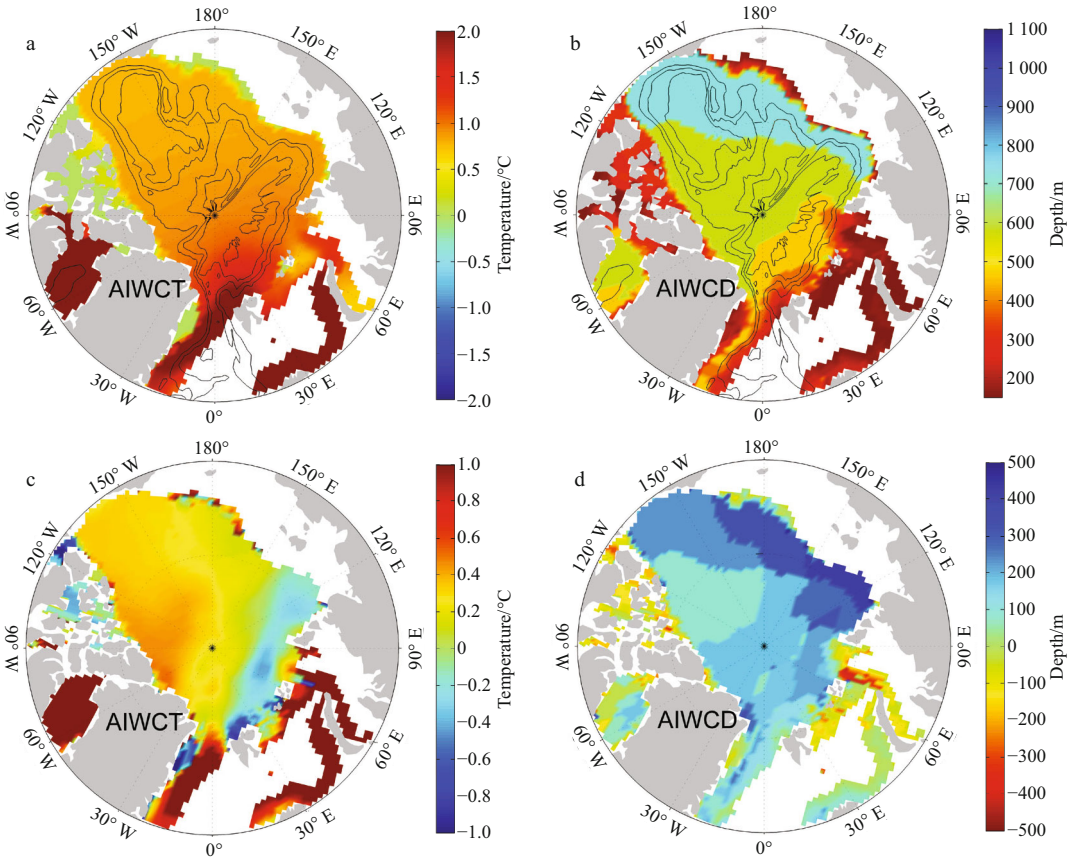

Fig.4. AIWCT (a) and AIWCD (b) of CCSM3, almost the same as Fig. 2 except for the data source, difference of AIWCT (c) (positive values mean AIWCT of CCSM3 is warmer) and AIWCD (d) (positive values mean AIWCD of CCSM3 is deeper).

ture. The nearly uniform 0.9–1°C of AIWCT throughout the Arctic Ocean means an underestimation in the Eurasian Basin and an overestimation in the Amerasian Basin. And the magnitudes of deviations in the Nansen Basin and the Canada Basin reach about –0.5 and 0.5°C, respectively. Another notable difference in the AIWCT is from the BSB. Large blank area in the Barents Sea shows a shallow warm water layer near the surface, which conflicts with the fact that Barents Sea is an active air-sea exchange region with the significant cooling process. Moreover, the extremely warm water over 2°C in the Barents Sea and even in the St. Anna Trough is a big deficiency of the model obviously, which suggests a clear heat supply from the BSB (also shown in Fig. 4b). That goes against the present knowledge of the heat supply of the AIW being mainly from the FSB (Section 3.2; see also Rudels, 2013). From the spatial pattern of the AIWCD, widely deepened AIW can be found with a scale of 200–400 m (Fig. 4d), which is a typical problem in the Arctic Ocean general circulation models (e.g., Li et al., 2011). In that paper, an excess of the vertical diffusion caused by the parameterization of the isopycnal diffusion was thought as the reason for this problem.

As detailed before, the CCSM4 has apparent improvements in ocean part and may be expected for a good representation of the AIW. But the results are rather frustrating (Fig. 5). The spatial distribution of the AIWCT is almost the same as that of the CCSM3 with all deficiencies existing. They are the misunderstanding the transport track of AIW in four basins, too warm water in the Barents Sea and misrepresenting the heat supply from the FSB and the BSB. However, there are some differences in spatial pattern of the AIWCD (Fig. 5b), though another incorrect pattern is generated. The AIWCD seems even worse in the CCSM4. The spatial distribution seems independent of the coverage of each basin, while in the CCSM3 it can obtain a shallower to deeper distribution from the Nansen Basin to the Canada Basin coarsely.

Results of some other CMIP5 models are also analyzed. The problem of the AIW in CCSM models is common for climate models (not shown). Recently, some modelers turned to the high resolution models and some got more realistic results (e.g., Aksenov et al., 2011). And the impact of the grid resolution on the simulated AIW was investigated by Li et al. (2013). Also, several ocean reanalyses have become more mature in these years, giving us a new tool to study the Arctic Ocean. Here we will provide the performances of two datasets with eddy-permitting ocean models and assimilation.

The SODA reproduces a relatively realistic spatial distribution of the AIWCT and the AIWCD in general with the warmest and shallowest AIW near the Fram Strait and the coldest and deepest in the Canada Basin (Fig. 6). The only significant errors of both AIWCT and AIWCD occur in the Eurasian Basin. The FSB does not flow as a boundary current along the slope of the Nansen Basin. Instead, it seems to turn to the interior in the western part of the Eurasian Basin and extend along the Lomonosov Ridge (Figs 6a and b). As a result, the AIW in the Amundsen Basin is abnormally warmer, while AIW at the east-

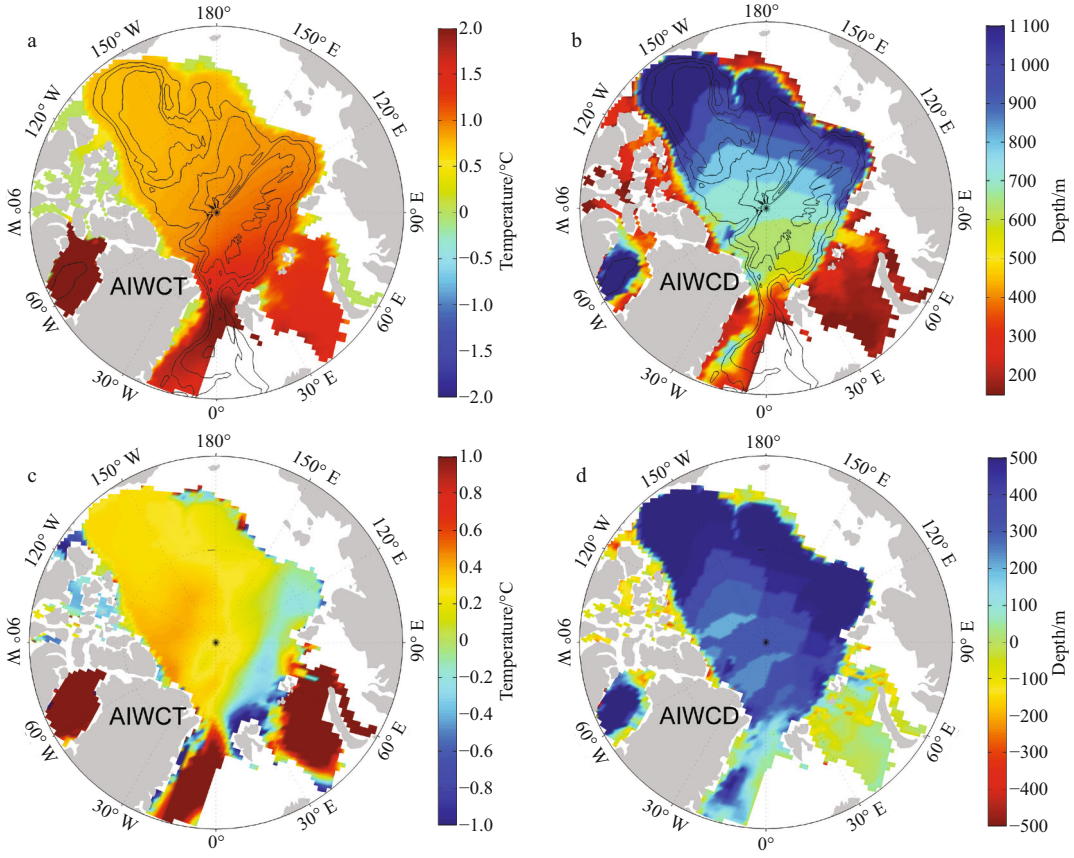

Fig.5. AIWCT (a) and AIWCD (b) of CCSM4, difference of AIWCT (c) and AIWCD (d) between CCSM4 and PHC. The same as Fig. 4 except for the data source.

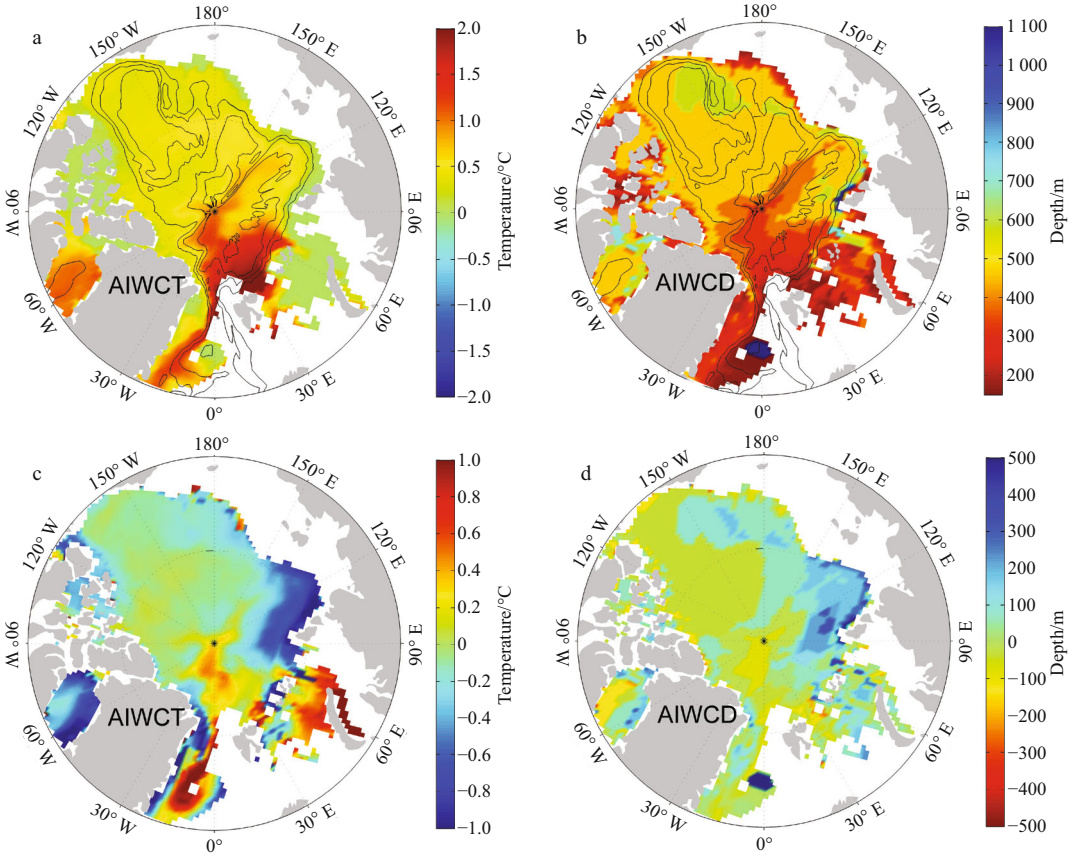

Fig.6. AIWCT (a) and AIWCD (b) of SODA, difference of AIWCT (c) and AIWCD (d) between SODA and PHC. The same as Fig. 4 except for the data source.

ern part of the Nansen Basin becomes colder than the PHC with a magnitude of over 0.5°C and deeper with a scale of 150–300 m. The spatial pattern is similar to the simulations of Li et al. (2011) and Li et al. (2013), suggesting a complicated problem of reproducing AIW in the eastern part of the Eurasian Basin, as also was mentioned by Lique and Steele (2012). They all suspected that misrepresentation of mixing process of the FSB and the BSB may be the main reason.

Climatological GLORYS AIWCT shows a striking cooling and deepening event in the Eurasian Basin (Fig. 7). The AIW in almost the whole Eurasian Basin is over 0.5°C cooler and 100 m deeper than the PHC, while it is the worst in the Nansen Basin where the AIWCT is over 1°C below PHC (Figs 7c and d). It is surprising that the AIWCT in the Fram Strait is a little higher than the PHC and has a sharp decline just north of the Svalbard. Since the FSB is the main source of heat of the AIW, the heat advected from the north Atlantic through the Fram Strait ought to play an importance role of maintaining the high temperature of the AIW. The transport in the Fram Strait will be discussed in the following section.

From the climatological spatial distributions of the AIWCT and the AIWCD, we find that the CCSM model without data assimilation drifts to a great extent and totally misrepresents the spatial pattern of the AIW. Two reanalyses also have some deficiencies. The AIW of the GLORYS with 0.5°C deviation in a large area can be regarded as a bad estimation, as the temperatures of water masses in polar regions are in a narrow range. The SODA obtains a best estimation among the three, though there are still some problems on the pathway of the extension of the AIW in the Eurasian Basin.

3.4 *Vertical profiles of temperature*

The vertical temperature structure of water column is another view of the reproducibility of the AIW. According to the partitions in Fig. 3 and the method mentioned in Section 3.1, the weighted average profiles in each partition are shown in Fig. 8. The AIWCTs of the PHC show a monotonous cooling distribution among the four basins with the AIWCDs deepening, as is coherent with the spatial patterns above. In general, compared with the PHC, the AIWs of climatology of the rest four datasets are thicker, which implies the excess vertical mixing of numerical models mentioned by Li et al. (2011).

The smooth curves of the temperature of two CCSM models seem to have too strong vertical mixing, especially in the Canada Basin (red lines, Partitions 8 and 9). The CCSM4 is surprisingly worst with the lower temperature at the intermediate depth and higher at the deep depth in all basins. The SODA conserves a best shape of the profile, while the temperature of the AIW in the eastern Eurasian Basin (Partitions 3 and 4) is the main discrepancy. For GLORYS, the low temperature in the Eurasian Basin is obvious, as is found above in the spatial distributions.

Loosely speaking, excessively strong vertical mixing does not

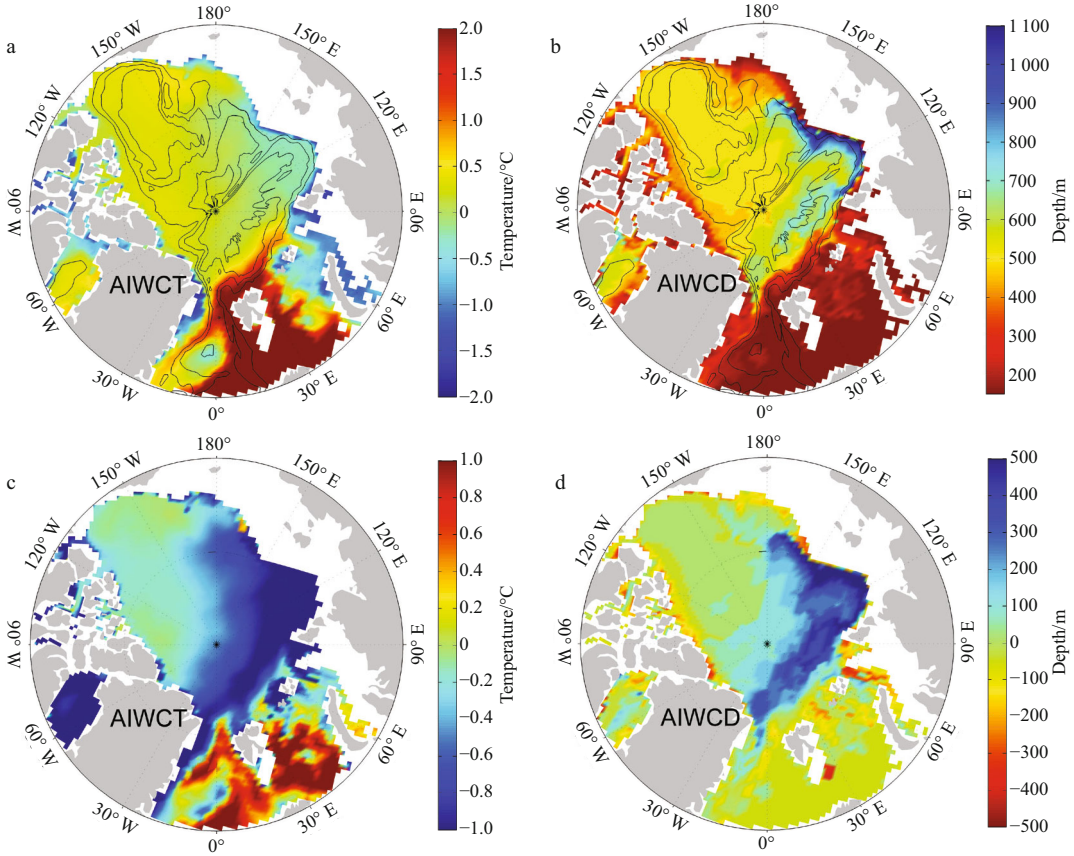

Fig.7. AIWCT (a) and AIWCD (b) of GLORYS, difference of AIWCT (c) and AIWCD (d) between GLORYS and PHC. the same as Fig. 4 except for the data source.

affect the total heat content of the water column. For a further description of the performance of datasets, we will calculate the heat content of the AIW in the next section.

3.5 *Heat content of AIW*

Figure 9 shows relative errors of each dataset. It is obvious that the CCSM3 and the CCSM4 are similar and both have positive errors in each partition. Note that even in the Nansen Basin (Partitions 1–4), the heat content of the CCSM is larger than the PHC while the AIWCT is lower (Figs 2c and 4c). That is to say, the Atlantic layer is thicker with a lower extremum, which implies the excess vertical mixing again. Except in the Nansen Basin, in all other basins, the relative errors exceed 1. That means the difference of the heat content can be as large as and even more than the AIW itself has actually. The largest error exists in the Canada Basin with the value more than 2. Because of the large area of the Canada Basin, the whole Arctic weighted average profile is influenced most by it. So the errors in the whole Arctic Basin (Partiton 10) also show a large positive value.

The climatological SODA is relatively delightful in relative errors. The largest error is below 1, which occurs in the Eurasian Basin. The result of relative errors of the heat content coincides with our comprehension of the spatial AIWCT. The opposite sign of errors of the western and eastern parts suggests the problem of the simulated pathway of the AIW. The abrupt change between Partitions 2 and 3 in accordance with the above text indicates the models' deficiency in the St. Anna Trough again.

The GLORYS exhibits negative errors almost in all partitions except 1. Values below –1 in the eastern part of the Nansen Basin and the Amundsen Basin (Partitions 3, 4, 5 and 6) reflect significant failure of reproduction of the warm character of AIW. The mean error of the Arctic Ocean (Partition 10) is nearly –1, which is several times larger than that of the SODA.

4 Movement and inflow of AIW

AIW is an alien of the Arctic Ocean. It comes from the north Atlantic Ocean with thermal property partly remained (e.g., Rudels et al., 1994). So the model performances of AIW can be affected by the simulated circulation patterns. In order to explain the spatial structures of AIW, we go a step further to investigate the circulation of the AIW layer in the Arctic Ocean and the velocity and transport at the entrance of FSB, the Fram Strait.

4.1 *Circulation of AIW layer in the Arctic Ocean interior*

Although there has been no available direct observation-based velocity field at the intermediate depth in the Arctic Ocean so far, basic knowledge of the circulation has been investigated in recent two decades by means of active tracers like temperature of warm AIW and passive tracers such as dissolved oxygen, silicon and radioactive pollutions (Rudels et al., 1994, 1999, 2012, 2013; Swift et al., 2007; Woodgate et al., 2001,

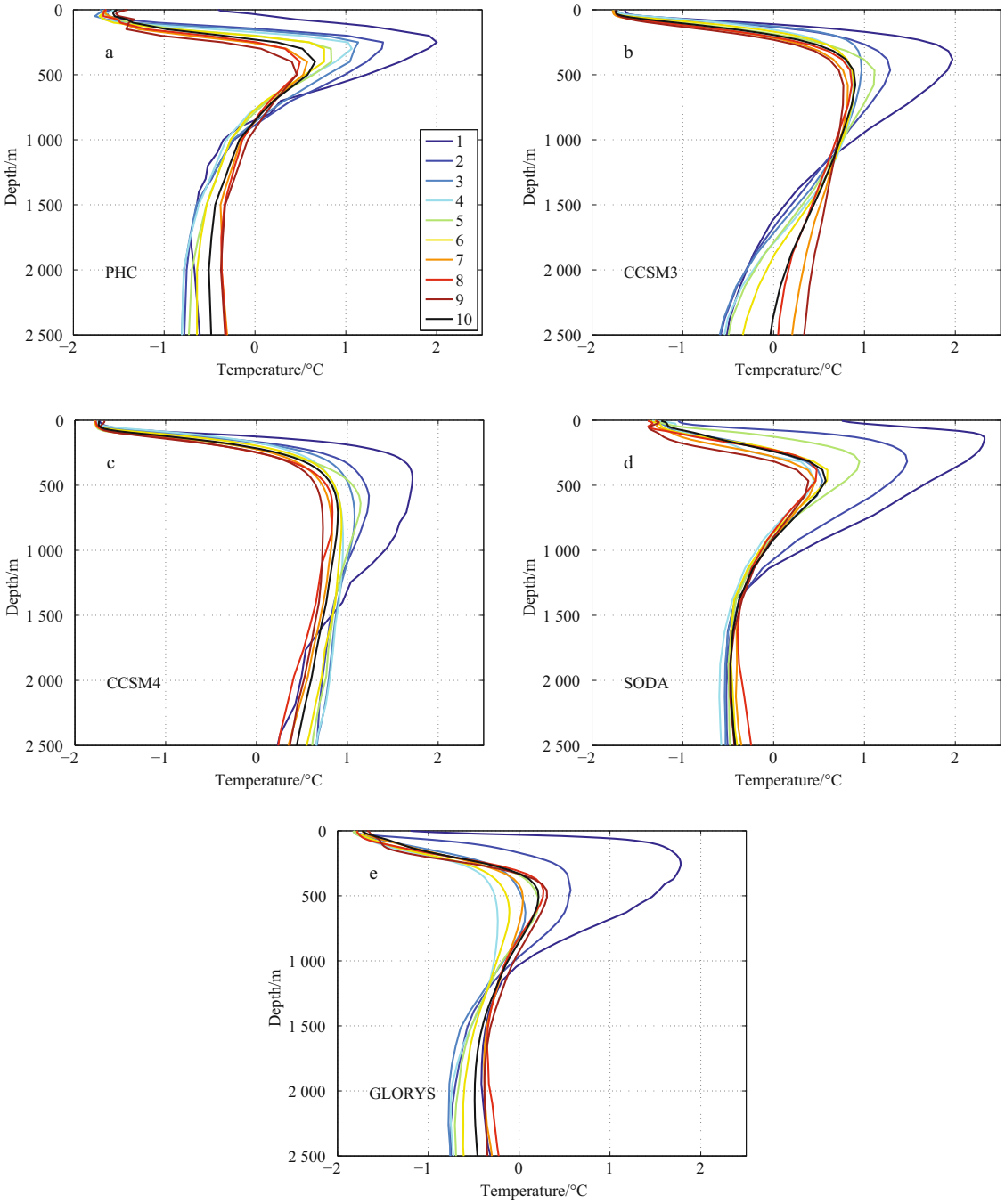

Fig.8. Vertical profiles of temperature in each partition according to Fig. 3. Data including PHC (a), CCSM3 (b), CCSM4 (c), SODA (d) and GLORYS (e) are climatology.

2007; Karcher et al., 2012). In those studies, they inferred that the ACBC is cyclonic in each basin from rare data, although the circulation of Atlantic water layer in the Canada Basin is still in debate. Also, Aksenov et al. (2011) illustrated the cyclonic movements of the three branches of the ACBC using a high resolution eddy-resolving model. The knowledge of cyclonic ACBC which carries Atlantic-origin water surrounding the slope of basin is commonly accepted, at least in the Eurasian Basin. For models, a reasonable circulation at the intermediate depth should be necessary to get a reasonable distribution of the AIW.

Figure 10 shows the vertical average of velocity of each dataset from 100 to 1 000 m (a vertical weighted average) using the same scale. Both CCSM models reproduce a weak circulation in the Arctic interior comparing to two reanalyses. The ACBC is hardly to distinguish with the velocity of boundary current less than 1cm/s in the Eurasian Basin, which is much slower than 6

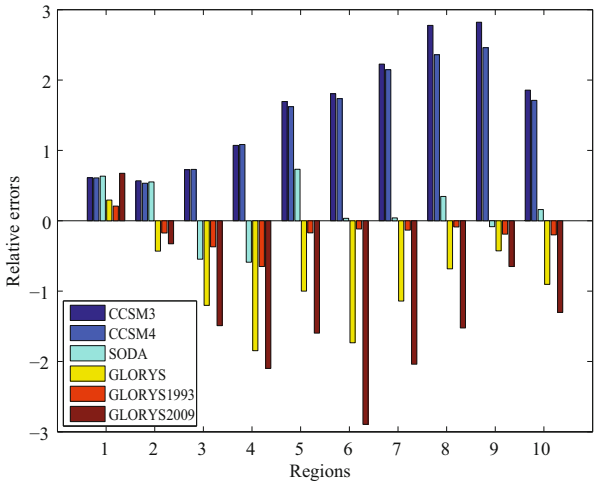

Fig.9. Relative errors of heat content of AIW in each partition, the region of each partition is shown in Fig. 3. Data used are climatology of datasets except the GLORYS1993 and GLORYS2009.

cm/s estimated by Lique and Steele (2012) from seasonal signal of Atlantic water and modeled result of about 5 cm/s according to Aksenov's (2011) simulation. Meanwhile, the northward West Spitsbergen Current (WSC) turns around almost totally at the Fram Strait as the re-circulation (Figs10a and b; see also Figs 11a and b). The FSB seems to be limited to the north of the Svalbard and no further extension can be found. However, a definite pathway of BSB can be easily found in the Barents and Kara Seas, forming a robust inflow at the St. Anna Trough. The circulation pattern explains the reason for the misrepresentation between the FSB and BSB mentioned in Section 3.2.

Both reanalyses successfully reproduce the cyclonic ACBC in the Eurasian Basin in a reasonable magnitude of 3–5 cm/s along the continental slope. Also the re-circulation at the Lomonosov Ridge is clear as some observations suggest (Woodgate et al., 2001). And GLORYS also reflects the topography constraint of the Gakkel Ridge, where a re-circulation is inferred from observations by Rudels et al. (2013). But the circulation in the Amerasian Basin seems a little rambling. In fact, the circulation at the intermediate depth in the Canada Basin is not fully understood for lack of *in situ* data. Karcher et al. (2012) pointed out that the extension of the Atlantic-origin water in the Canada Basin might not as steady as we thought traditionally. The FSB

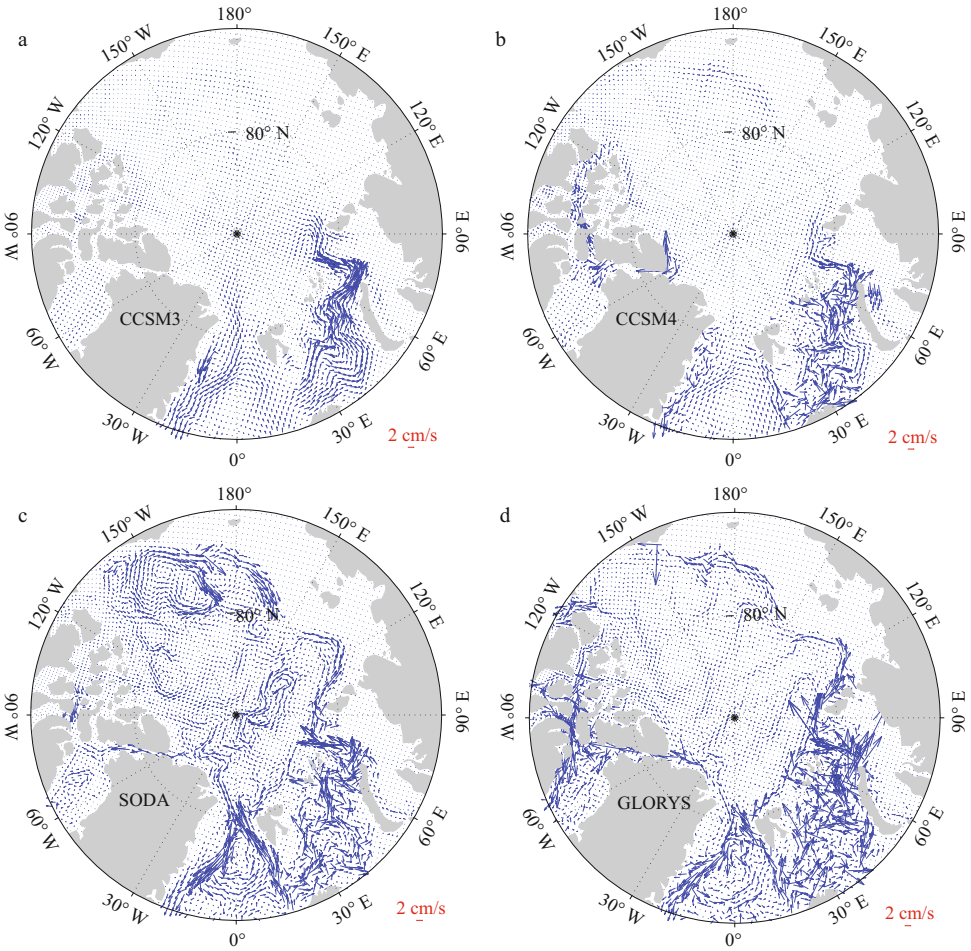

Fig.10. Vertical average of velocity of each dataset ranging from 100 to 1 000 m, CCSM3 (a), CCSM4 (b), SODA (c) and GLORYS (d).

is much more realistic in the SODA and the GLORYS. A robust inflow in the Fram Strait can be found and the inflow Atlantic water goes along the slope as the FSB of the ACBC, which is lost in CCSM models.

Although the data simulation of the temperature and the salinity is a positive factor of the modeled circulation for some dynamical reasons, e.g., the thermal wind relation, it may be not the key factor of the reproducibility of the circulation of two reanalyses. We suppose that the differences of this issue can be attributed to the horizontal resolution as mentioned by Li et al. (2013), who illustrated the impact of the horizontal resolution on the modeled AIW by a series of sensitive experiments. The eddy-permitting resolution of the SODA and the GLORYS is of great importance to represent the mesoscale eddies and the eddy-topography interaction. So it is a credible explanation why the non-eddy-permitting CCSM climate models fail to reproduce the topography steered boundary current.

4.2 *Velocity, temperature and transport in the Fram Strait*

The Fram Strait is the only deep channel where the water in the Arctic Ocean exchanges with other oceans. The advection heat input through the Fram Strait is an important factor influencing the AIW, at least in the Eurasian Basin. So the details in the Fram Strait need to be analyzed particularly for the focus of this paper in order to understand the deficiencies of the AIW's performances in these datasets.

Because there are direct observations from mooring arrays in the Fram Strait since 1997 (Fahrbach et al., 2001; Schauer et al., 2004; Schauer et al., 2008), we use the figures and statistical values from mooring data to evaluate the models' simulations instead of the PHC. The model data are interpolated onto the section of 78°50′N where the moorings were deployed.

The temperature distributions in the section in each dataset (Fig. 11, black contours) are compared with Fig. 3.2 in Schauer et al. (2008) and Fig. 2 in Beszczynska-Moller et al. (2012). All four datasets capture the basic pattern with the warm Atlantic water at the upper and intermediate depths in the eastern part of the Fram Strait, the cold water from the Arctic Ocean in the western part, and the relative cool water below 1 000 m supplying the deep part of the strait. The distributions of the temperature of two reanalyses are similar to observations in general, but those are a little more different in both CCSM models. The 0 isothermal is at about 900 m in observations and roughly at 1 000 m in the SODA and the GLORYS. The 0 isothermals in both CCSM models are suppressed to deeper depths. It appears at 1 500 m in the CCSM3 and is missing in the CCSM4, which implies a too thick warm Atlantic water layer. This is because almost the whole WSC recirculates without entering the Arctic Ocean in both CCSM models (Figs 10a and b). While in two reanalyses the extensions of the WSC in the form of the FSB are robust.

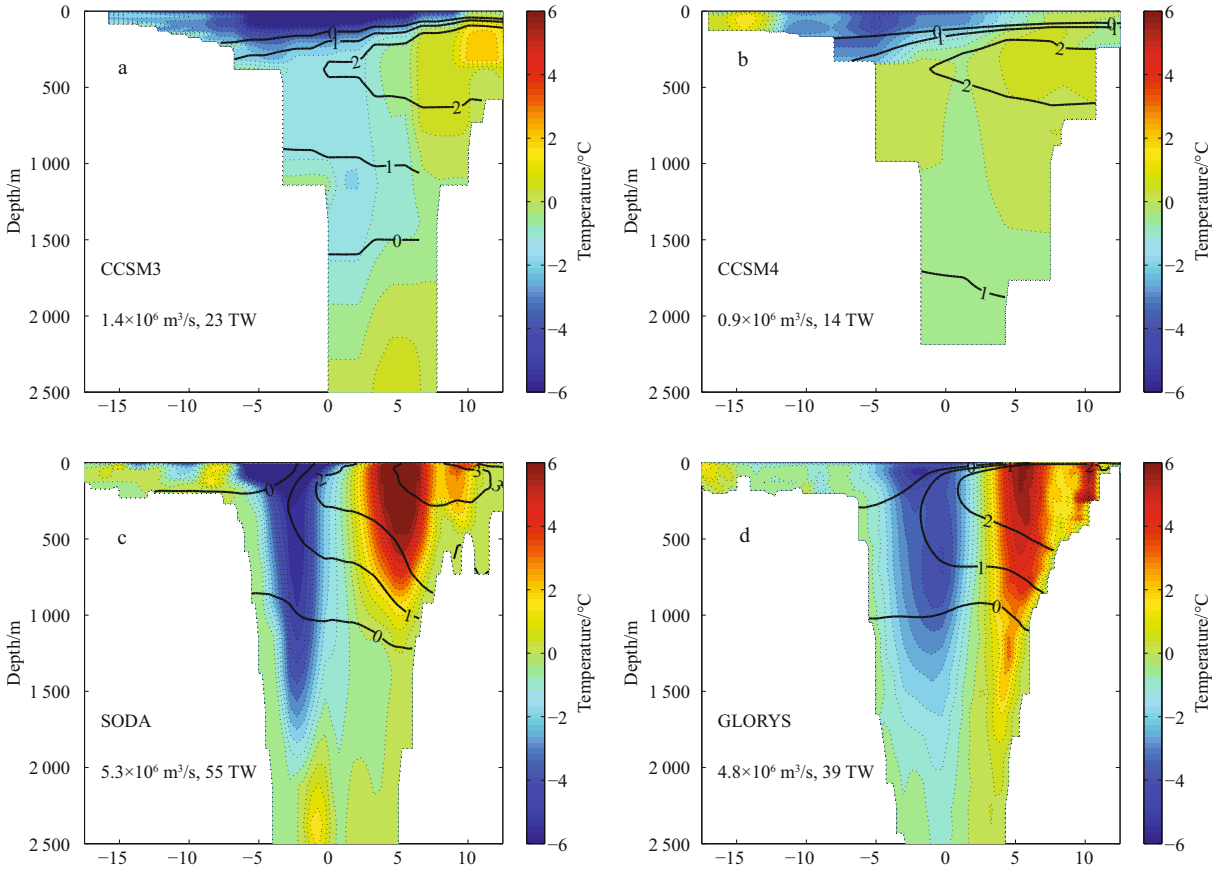

Fig.11. Velocity (color shading, northward positive) and temperature (black solid contour) of each dataset in the Fram Strait. Also the northward volume transport and heat transport (TW, 1 TW=10^{12} W) referring to 0°C are listed.

The recirculated Atlantic water has a relatively higher temperature than the transformed water after undergoing mixing in the Arctic Ocean. Compared with the observations, the maximum temperature of Atlantic water seems to be underestimated in all modeled datasets. Another difference in the CCSM3 is a thicker (about 60 m) polar surface layer in the eastern part of the strait, which does not exist in the observation and two reanalyses. A possible explanation may be that the coupled climate models' air-ice-sea exchange process in the CCSM may more easily drift from the reality, while the surface fluxes of reanalyses are fixed to atmospheric reanalyses and the SST is assimilated by the satellite-origin observational data.

The distributions of the cross-strait velocity also have a similar pattern among the models and observations though the magnitudes differ. The WSC in the CCSM3 and the CCSM4 is only 2 cm/s. A significant stronger WSC inflow with maximum speed of 8 and 6 cm/s is reproduced in the SODA and the GLORYS respectively. However, the modeled velocity in the eastern part of the strait is much slower than the observation of 20–30 cm/s (Fig. 3.2 in Schauer et al., 2008). According to their mooring observation, the velocity field is very complex with several alternative barotropic belts zonally. It is evident that the coarse climate CCSM3 models have little possibility to reproduce the realistic velocity field. In spite of underestimation in the SODA and the GLORYS, the eddy-permitting ocean models indeed generate a more realistic velocity field, which agrees with the conclusion of Li et al. (2013). In addition, the barotropic structure is also more robust in two reanalyses than that in CCSM. It occurs not only in the eastern part, but also in the western part where the southward East Greenland Current (EGC) carries the water out of the Arctic Ocean.

The northward volume transport in the Fram Strait is another benchmark for the inflow of Atlantic water. 1.4×10^6 and 0.9×10^6 m^3/s in CCSM3 and CCSM4 models is one order of magnitude lower than observations 9×10^6–10×10^6 m^3/s (Schauer et al., 2004) and 12×10^6 m^3/s (Schauer et al., 2008). The slow cross-strait velocity should be the main cause for almost one order of underestimation (Figs 11a and b). The northward volume transport is larger in the SODA and the GLORYS to some extent, being 5.3×10^6 and 4.8×10^6 m^3/s respectively, though they are still underestimations of nearly half of the observations. These results seem to be related to the horizontal resolution. According to the inference of Li et al. (2013), the non-eddy-permitting models tend to misunderstand the inflow of the Atlantic water, meaning an underestimation in the Fram Strait and an overestimation in the Barents Sea Opening (BSO) (Figs 11a and b, see also the circulation in Figs 10a and b), which agrees with the results of other ocean models (Golubeva, oral report in AOMIP Workshop; Aksenov, personal communication). The eddy-permitting models can generate a larger transport, while the inflow in the BSO is still too large (not shown, but reflected in Figs 10c and d) according to the observations that indicated the inflow in the Fram Strait is roughly five times larger than that in the BSO (Schauer et al., 2004; Schauer et al, 2008; Skagseth et al., 2008; Smedsrud et al., 2010).

The heat transport is a combined contribution of the temperature and the velocity. However, the calculation of the heat transport is a puzzling question and may vary a lot due to different artificial reference temperatures (Schauer et al., 2008). Here we do not focus on the method of the calculation and use a similar method like that of Schauer et al. (2004). The heat transports of 23 TW in the CCSM3 and 14 TW in the CCSM4 respectively are obvious lower than 32 to 55 TW of observations (Schauer et al., 2004). It is surprising that both CCSM models overestimate the heat content of the AIW in the Arctic interior (see Fig. 9). On these grounds, we affirm that the huge heat content of the AIW in the CCSM is mainly supplied by the BSB, which is far from known knowledge. The transports of both reanalyses (55 and 39 TW) fall in the realistic range. Note that the realistic heat transport versus half of the realistic volume transport implies that the temperature in the Fram Strait (especially in the eastern part) in two reanalyses is higher than observations. Since both reanalyses reproduce a reasonable heat input, the great differences of heat content of the AIW between the SODA and the GLORYS seem interesting. This will be discussed next.

5 Impact of data assimilation on two reanalyses

The two reanalyses SODA and GLORYS have similar horizontal resolution. Both circulation patterns fall in a reasonable range as expected. In addition, the inflow velocity, temperature, volume and heat transports are also close to the other. So a question must arise. Why their performances of the AIW differ significantly? We try to answer it from the impact of the data assimilation.

As mentioned above, the data sources of assimilation in two reanalyses differ with a remarkable characteristic that no *in situ* observations of the Arctic Ocean are included in the GLORYS. So GLORYS can be regarded as a free simulation in the Arctic Ocean with a realistic "open boundary" at the rest of the global ocean, while the SODA is a fixed simulation with assimilation. Considering the realistic heat input of the North Atlantic through the Fram Strait, we attribute the failure of reproducing the AIW in the GLROYS to intrinsic deficiencies of model's reproducibility. The ocean model of the GLORYS is not able to maintain the high temperature of the AIW. Meanwhile, there are no essential differences in model physics, numeric methods and grid resolutions between the ocean models of the SODA and the GLORYS. We suppose that the relatively reasonable AIWCT in the SODA is with the help of assimilation, which acts as a heat source to the modeled AIW.

Figure 12 provides an evidence for the impact of the data assimilation. From the spatial patterns of the AIWCT of adjacent two months of the year 1993, abnormal warm water is found in the eastern part of the Eurasian Basin. Considering the heat content of the AIW is totally from the North Atlantic inflow, this warm water should be transported by the ACBC from an upstream position. This water parcel is supposed to be at north of the Kara Sea in July, which is the nearest area with the AIWCT over 1.5°C. A displacement of the water parcel during 1 month implies a steady velocity more than 20 cm/s, which is nearly one order higher than existing estimations (e.g., Aksenov et al., 2011). The only explanation is the abnormal heat content in August in the eastern part of the Eurasian Basin is introduced artificially by assimilation data. Because of nonuniform data of the assimilation in space and time, this warm event is not reproduced in the upstream region in July. Actually, a strong warming event in the early 1990s did occur originating in the Fram Strait and was found later in downstream regions (Quadfasel et al., 1991; Grotefendt et al., 1998; Woodgate et al., 2001). This unaccountable phenomenon in the SODA indicates that the ocean model itself cannot capture this warming event without assimilation. That is to say, the artificial heat input is of great impor-

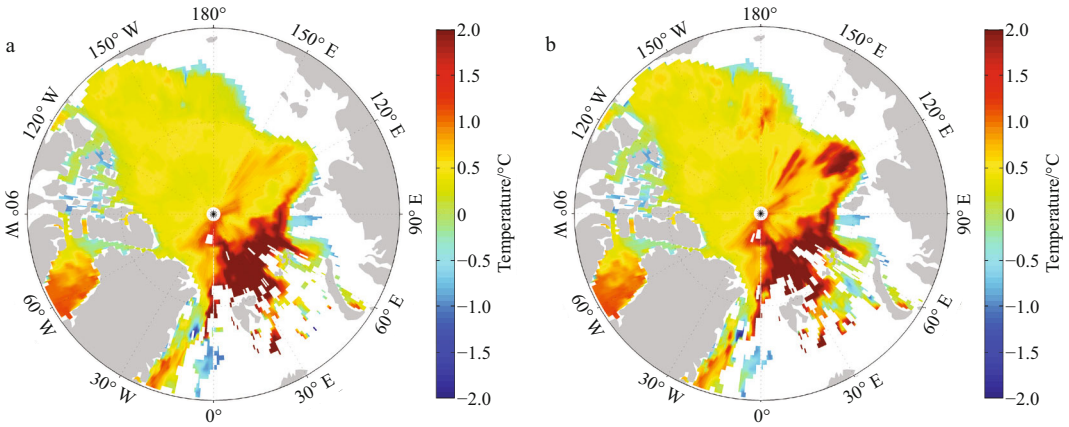

Fig.12. Distribution of AIWCT in July (a) and August (b) 1993 of SODA.

tance to the balance of heat content of the AIW in the SODA.

On the contrary, the freely simulated GLORYS drifts dramatically. Let us revisit the heat content in Fig. 9. The last two samples are calculated from the annual mean data of year 1993 and 2009. It exhibits a good performance generally at the beginning of the dataset in 1993 with errors below 0.5 in almost all partitions except 4. However, the model of the GLORYS drifts obviously within its 17 years run. The AIW in most parts of the Arctic Ocean undergoes a remarkable cooling process. Values of less than –1 in many partitions and the whole basin (Partition 10) mean a huge heat loss. The extremum over –2 in western part of the Eurasian Basin implies the AIW in that region has totally lost its intrinsic characteristic in 2009. The "climatology values" are between those of the year 1993 and 2009 in almost all partitions, providing an evidence of the model drift of the GLORYS.

This drift does not occur in the SODA during its 50 years simulation (not shown). In summary, it is plausible that the input heat from assimilation not only acts as a heat source to the AIW, but also helps to avoid the drift of the simulated AIW.

6 Conclusions and discussion

In this paper, the simulations of the AIW in four datasets are analyzed. Relative to the PHC data, Climate CCSM models do not reproduce reasonable spatial patterns of the AIWCT and the AIWCD with widespread biases of 0.5°C and over 200 m, while the heat contents of all basins are overestimated with an over a 1.5 basin-average relative error. The opposite signs of biases of the AIWCT and the heat content imply an unrealistic thicker Atlantic layer. The main defect is it misunderstands contributions of the FSB and the BSB. The simulated BSB in CCSMs is too robust while in the Fram Strait the volume transports are roughly one order weaker than observations. Among these four datasets, the SODA has the best representation of spatial pattern of AIW temperature and depth with biases less than 0.5°C and 150 m except in the eastern part of the Eurasian Basin. The relative errors of heat content are below 1 in all regions. The AIW in the GLORYS has an obvious drift. The climatological spatial patterns show over 0.5°C cooler and 100 m deeper deviation in the whole Eurasian Basin and the values can reach 1°C and 200 m in the Nansen Basin. The heat content of the GLORYS at the beginning of the time range is quite well with less than 0.5 relative errors in all basins. But the heat content cannot maintain with –1 relative error in most regions and over –2 in western part of the Eurasian Basin at the end of the time range, suggesting that the characteristic of the AIW is totally lost especially in the Eurasian Basin. From vertical profiles of the temperature, thicker AIWs are found in all four datasets comparing with the PHC, which may be the result of excess vertical mixing.

The horizontal resolution is likely to be important in the simulation of circulation of the Atlantic water at the intermediate depth. Both eddy-permitting ocean models of the SODA and the GLORYS reproduce a strong cyclonic circulation at the intermediate depth in the Eurasian Basin while the circulations in non-eddy-permitting CCSM models are much weaker. Also, the constraint of topography in two reanalyses is clear. The inflow of the Atlantic-origin water in the Fram Strait in two higher resolution models is much higher, in spite of underestimating, than that in the CCSMs. The small Rossby deformation radius in the Arctic Ocean is thought to be an explanation for the differences. The potential vorticity (PV) balance theory can successfully explain the circulation in the Arctic Ocean among ocean general models (Yang, 2005; Karcher et al., 2007). The effect of the horizontal resolution can also be attributed to it. The fine resolution at the slope can resolve the dissipation effect of the velocity viscosity. The PV budget can be more realistic. This issue was discussed and parameterized as the Neptune parameterization (Holloway, 1986; Holloway and Wang, 2009). The effects of this parameterization on the Atlantic water circulation and water properties were investigated by Golubeva and Platov (2007), Holloway et al. (2007), Wang et al. (2011) and Li et al. (2013). They all showed positive aspects of this parameterization. The Neptune parameterization was concluded to an effective method for the coarse models to represent the eddy-topography interaction.

It is suggested that the artificial heat input from data assimilation in the SODA accounts for the obvious different performances of the AIW between the SODA and the GLORYS. By analyzing the spatial pattern of the AIWCT in 1993, a clear evidence of this heat input is found in the SODA. From this study, the irreproducibility of the modeled AIW in present ocean general circulation models is revealed. More efforts need to be made to improve the comprehension and parameterizations of physical processes in the Arctic Ocean.

References

Aksenov Y, Ivanov V V, Nurser A J G, et al. 2011. The arctic circumpolar boundary current. J Geophys Res, 116: C09017

Beszczynska-Moller A, Fahrbach E, Schuaer U, et al. 2012. Variability in Atlantic water temperature and transport at the entrance to the Arctic Ocean, 1997–2010. ICES Journal of Marine Science, 69(4): doi: 10.1093/icesjms/fss056

Carton J, Giese B. 2008. A reanalysis of ocean climate using simple ocean data assimilation (SODA). Mon Wea Rev, 136: 2999–3017

Collins W, Bitz C, Blackmon M, et al. 2006. The community climate system model version 3 (CCSM3). J Climate, 19: 2122–2143

Dmitrenko I A, Kirillov S A, Serra N, et al. 2014. Heat loss from the Atlantic water layer in the St. Anna trough (northern Kara Sea): causes and consequences. Ocean Sci Discuss, 11: 543–573

Fahrbach E, Meincke J, Østerhus S, et al. 2001. Direct measurements of volume transports through Fram Strait. Polar Res, 20(2): 217–224

Ferry N, Parent L, Garric G, et al. 2012. GLORYS2V1 global ocean reanalysis of the altimetric era (1992–2009) at meso scale. Mercator Quarterly Newsletter, 44: 29–39

Gent P R, McWilliams J C. 1990. Isopycnal mixing in ocean circulation models. J Phys Oceanogr, 20(1): 150–155

Golubeva E N, Platov G A. 2007. On improving the simulation of Atlantic water circulation in the Arcitc Ocean. J Geophys Res, 112: C04S05

Grotefendt K, Logemann K, Quadfasel D, et al. 1998. Is the Arctic Ocean warming? J Geophy Res, 103(C12): 27679–27687

Holloway G. 1986. A shelf wave/topographic pump drives mean coastal circulation. Ocean Modelling, 68: 12–15

Holloway G, Dupont F, Golubeva E, et al. 2007. Water properties and circulation in Arctic Ocean models. J Geophys Res, 112: C04S03

Holloway G, Wang Z. 2009. Representing eddy stress in an Arctic Ocean model. J Geophys Res, 114: C06020

Ivanov V V, Alexeev V A, Repina I A, et al. 2012. Tracing Atlantic water signature in the arctic sea ice cover east of Svalbard. Advances in Meteorology, 2012: 201818, doi: 10.1155/2012/201818

Karcher M, Kauker F, Gerdes R, et al. 2007. On the dynamics of Atlantic water circulation in the Arctic Ocean. J Geophys Res, 112: C04S02

Karcher M, Smith J, Kauker F, et al. 2012. Recent changes in Arctic Ocean circulation revealed by iodine-129 observations and modeling. J Geophys Res, 117: C08007

Large W G, McWilliams J C, Doney S C. 1994. Oceanic vertical mixing: a review and a model with a nonlocal boundary layer parameterization. Reviews of Geophysics, 32(4): 363–403

Li Shujiang. 2008. A study on the arctic intermediate water's spatial distribution, temporal change and its dynamical process [dissertation] (in Chinese). Qingdao: Ocean University of China

Li Shujiang, Zhao Jingping, Su Jie, et al. 2012. Warming and depth convergence of the arctic intermediate water in the Canada basin during 1985–2006. Acta Oceanol Sin, 31(4): 46–54

Li Xiang, Su Jie, Zhang Yang, et al. 2011. Discussion on the simulation of arctic intermediate water under Nemo framework. In: Proceedings of Twentieth (2011) International Offshore and Polar Engineering Conference. Vol. 1. Hawaii: the International Society of Offshore and Polar Engineers (ISOPE), 953–957

Li Xiang, Su Jie, Wang Zeliang, et al. 2013. Modeling arctic intermediate water: the effects of Neptune parameterization and horizontal resolution. Adv Polar Sci, 24(2): 98–105

Lique C, Steele M. 2012. Where can we find a seasonal cycle of the Atlantic water temperature within the Arctic Basin. J Geophys Res, 117: C03026

Madec G. 2008. Nemo ocean engine. note du Pole de modélisation, Institut Pierre-Simon Laplace (IPSL), France

Madec G, Delecluse P, Imbard M, et al. 1998. OPA 8.1 ocean general circulation model reference manual. Note du Pole de modélisation, Institut Pierre-Simon Laplace (IPSL)

McLaughlin F A, Carmack E C, Williams W J, et al. 2009. Joint effects of boundary currents and thermohaline intrusions on the warming of Atlantic water in the Canada Basin, 1993–2007. J Geophys Res, 114: C00A12

Pachauri R K, Reisinger A. 2007. Climate change 2007: synthesis report. In: Contribution of Working Groups I, II and III to the Fourth Assessment Report of the Intergovernmental Panel on Climate Change. Geneva, Switzerland: IPCC

Polyakov I V, Alekseev G V, Timokhov L A, et al. 2004. Variability of the intermediate Atlantic water of the Arctic Ocean over the last 100 years. J Climate, 17: 4485–449

Polyakov I V, Alexeev V V, Ashik I M, et al. 2011. Fate of early-2000s arctic warm water pulse. Bulletin of the American Meteorological Society, 92(5): 561–566

Quadfasel D A, Sy A, Wells D, et al. 1991. Warming in the arctic. Nature, 350(6317): 385

Rudels B, Jones E P, Anderson L G, et al. 1994. On the intermediate depth waters of the Arctic Ocean. In: The Polar Oceans and Their Role in Shaping the Global Environment: The Nansen Centennial Volume. Geophys Monogr Ser, 85. Washington DC: AGU, 33–46

Rudels B, Anderson L G, Jones E P. 1996. Formation and evolution of the surface mixed layer and halocline of the Arctic Ocean. J Geophys Res, 101(C4): 8807–8821

Rudels B, Friedrich H J, Quadfasel D. 1999. The arctic circumpolar boundary current. Deep-Sea Research Part II, 46(6–7): 1023–1062

Rudels B, Jones P E, Schauer U, et al. 2004. Atlantic sources of the Arctic Ocean surface and halocline waters. Polar Research, 23(2): 181–208

Rudels B, Schauer U, Bjork G, et al. 2013. Observations of water masses and circulation with focus on the Eurasian basin of the Arctic Ocean from the 1990s to the late 2000s. Ocean Sci, 9: 147–169

Rudels B. 2013. Arctic Ocean circulation, processes and water masses: a description of observations and ideas with focus on the period prior to the International Polar Year 2007–2009. Progress in Oceanography, doi: 10.1016/j. pocean.2013.11.006

Schauer U, Fahrbach E, Østerhus S, et al. 2004. Arctic warming through the Fram Strait: oceanic heat transport from 3 years of measurements. J Geophys Res, 109: C06026

Schauer U, Beszczynska-Moller A, Walczowski W, et al. 2008. Variation of measured heat flow through the Fram Strait between 1997 and 2006. In: Dickson R R, Meincke J, Rhines P, eds. Arctic–Subarctic Ocean Fluxes: Defining the Role of the Northern Seas in Climate. Dordrecht: Springer, 65–85

Skagseth O, Furevik T, Ingvaldsen R B, et al. 2008. Volume and heat transports to the Arctic Ocean via the Norwegian and Barents seas. In: Dickson R R, Meincke J, Rhines P, eds. Arctic-Subarctic Ocean Fluxes: defining the role of the Northern Seas in climate. Dordrecht: Springer, 45–64

Smedsrud L H, Ingvaldsen R, Nilsen J E, et al. 2010. Heat in the Barents Sea: transport, storage, and surface fluxes. Ocean Science, 6: 219–234

Smith R, McWilliams J C. 2003. Anisotropic horizontal viscosity for ocean models. Ocean Modelling, 5: 129–156

Steele M, Boyd T. 1998. Retreat of the cold halocline layer in the Arctic Ocean. J Geophys Res, 103(C5): 10419–10435

Steele M, Morley R, Ermold W. 2001. PHC: a global ocean hydrography with a high quality Arctic Ocean. J Climate, 14: 2079–2087

Wang Z, Holloway G, Hannah C. 2011. Effects of parameterized eddy stress on volume, heat, and freshwater transports through Fram Strait. J Geophys Res, 116: C00d09

Woodgate R, Aagaard K, Muench R D, et al. 2001. The Arctic Ocean boundary current along the Eurasian slope and the adjacent Lomonosov Ridge: water mass properties, transports and transformations from moored instruments. Deep-Sea Research I, 48(8): 1757–1792

Woodgate R A, Aagaard K, Swift J H, et al. 2007. Atlantic water circulation over the Mendeleyev ridge and Chukchi borderland from thermohaline intrusions and water mass properties. J Geophys Res, 112: C02005

Yang J. 2005. The arctic and subarctic ocean flux of potential vorticity and the Arctic Ocean circulation. J Phys Oceanogr, 35(12): 2387–2407

Zhong Wenli, Zhao Jinping. 2014. Deepening of the Atlantic Water Core in the Canada Basin in 2003-11. J Phys Oceanogr, 44(9): 2353–2369